

Mechanistic Study of the Peroxidase-Catalyzed Polymerization of Sulfonated Phenol[†]

Wei Liu, Ashok L. Cholli,* Jayant Kumar, and Sukant Tripathy

Center for Advanced Materials, Departments of Chemistry and Physics,
University of Massachusetts Lowell, Lowell, Massachusetts 01854

Lynne Samuelson*

Natick Soldier Center, U.S. Army Soldier and Biological Chemical Command,
Natick, Massachusetts 01760

Received November 27, 2000; Revised Manuscript Received March 13, 2001

ABSTRACT: Peroxidase-catalyzed polymerization of sulfonated phenol was investigated by ¹H and ¹³C NMR spectroscopy. The reaction process was monitored by ¹H NMR spectroscopy with the incremental addition of H₂O₂. The variation of the dimer concentration shows three different stages during the reaction: proliferation (I), equilibrium (II), and reduction (III) of the dimer. Conversion of most of the monomer is devoted to the formation of small molecular weight species such as dimers at stage I. A dynamic equilibrium exists between the formation and consumption of the dimer in the reaction system at stage II. The likelihood of formation of high molecular weight products increases at stage III. Structural characterizations of the predominant dimer product and the resulted polymer suggest that C–O–C coupling is dominant in the polymerization, leading to the synthesis of a polymeric material with sulfonated phenylene oxide as the major unit.

Introduction

Enzyme-based polymerization as a new biotechnological methodology in the polymer synthesis has attracted a lot of interest due to the environmental compatibility and possibility of producing polymer in high yield.¹ Recently, peroxidase-catalyzed oxidative polymerization of phenols and anilines has been extensively explored in the conditions including solvents mixtures,² modified monomers in aqueous solutions,³ micelles,⁴ reverse micelles,⁵ and polymerizations at the air–water interface⁶ and in the presence of a template.⁷ The synthesized polyanilines and polyphenols show interesting optical and electrical properties with potential applications in the fabrication of optical and electronic devices.^{2c,7}

Typically, peroxidase-catalyzed polymerization of phenol is carried out in the presence of H₂O₂. The catalytic cycle of peroxidase involves a two-electron oxidation step and two one-electron reduction steps, resulting in the formation of phenolic radicals.⁸ These free radicals then undergo coupling to produce the dimer, and successive oxidation and coupling and transfer reactions eventually result in the formation of polymer. In this process, the generation of radical is enzyme-dependent. However, radical–radical coupling and transfer are controlled exclusively by the phenoxy radical and solvent chemistries.⁹ The peroxidase-catalyzed polymerization of phenol and its various derivatives usually produce the polymers with a complicated structure. The main structure was estimated to be of phenylene units or a mixture of phenylene and oxyphenylene units.^{2a,e} Very limited nuclear magnetic resonance (NMR) spectroscopy research on peroxidase-catalyzed polymerization has been reported.¹⁰ In the present work, the process and detailed

coupling mechanism of peroxidase-catalyzed polymerization of sulfonated phenol are investigated by NMR spectroscopy.

Experimental Section

Materials. Horseradish peroxidase (HRP) (EC 1.11.1.7) (200 unit/mg) was purchased from Sigma Chemicals Co., St. Louis, MO, with RZ > 2.2. A stock solution of 10 mg/mL in pH 6.0, 0.1 M phosphate buffer was prepared. The monomer 4-hydroxybenzenesulfonic acid, sodium salt dihydrate, was obtained from Aldrich Chemicals Co. Inc., Milwaukee, WI, and used as received. All other chemicals and solvents used were also commercially available, of analytical grade or better, and used as received.

Enzymatic Polymerization. The peroxidase-catalyzed polymerization was performed in a 100 mL, 0.1 M, pH 6.0–7.0 phosphate buffer solution containing 0.1 M sulfonated phenol and 0.1 mg/mL HRP. Equal molar H₂O₂ was pumped separately over a period of 3 h into the reaction mixture. The solution was stirred for an additional 12 h after all of the H₂O₂ was added. The final reaction solution was purified by ultrafiltration with the Spectrum MiniKros sampler system using the MiniKros sampler UF module with 10 kDa molecular weight cutoff to remove the monomer and oligomer. The resulted solution was dried at room temperature, and the collected powder was vacuum-dried for another 24 h.

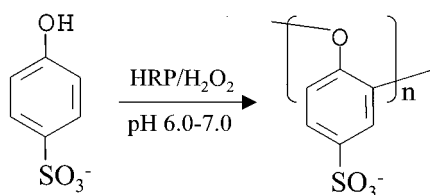
¹H NMR of Enzymatic Polymerization. Sequential NMR spectra were recorded on a Bruker ARX 500-MHz NMR spectrometer during the process of HRP-catalyzed polymerization of sulfonated phenol with the similar condition as described above. To an NMR tube was transferred 0.6 mL of 0.1 M, pH 6.0 phosphate buffer solution containing 4.64 mg of monomer, 0.3 mg of HRP, and 0.3 mg of pyrazine (internal standard). In this case, the buffer solution is prepared by dissolving phosphate sodium salt into D₂O. Before the initiation of the reaction, a ¹H NMR spectrum is taken. After each addition of 5 μ L of H₂O₂ (0.5 M in D₂O) to the NMR tube, the solution was thoroughly mixed, and another NMR spectrum was taken 5 min later.

¹H and ¹³C NMR of Polymer. ¹H and ¹³C NMR spectra of the polymer were also recorded on the Bruker ARX 500-MHz

[†] This paper is dedicated in the memory of Prof. Sukant Tripathy.

* To whom all correspondence should be addressed.

Scheme 1



NMR spectrometer. The sample was prepared by dissolving the purified enzymatically synthesized sulfonated polyphenol powder (0.2 g) in 0.6 mL of D₂O.

Results and Discussion

HRP-catalyzed polymerization of sulfonated phenol (4-hydroxybenzenesulfonic acid, sodium salt dihydrate) is performed in 0.1 M phosphate buffer solution at pH 6.0–7.0 as schematically depicted in Scheme 1. Equal molar H₂O₂ is added gradually to the reaction mixture containing HRP and the monomer. Gradual addition of H₂O₂ is necessary to avoid the inhibition of HRP often caused by high concentration peroxide^{2a} and to manipulate the reaction rate by controlling the addition of H₂O₂ into the reaction system. The whole process of this enzyme-catalyzed polymerization of sulfonated phenol is monitored by ¹H NMR spectroscopy. Figure 1 shows the stack plots of ¹H NMR spectra of the reaction mixture containing sulfonated phenol and HRP before (a) and after 5 min of each incremental addition of H₂O₂ (b–i). No significant spectrum changes are observed after 5 min, indicating that the reaction is very close to the final product distribution at that time. To obtain quantitative information on the conversion of monomer and the formation of products, pyrazine, a symmetric molecule (does not participate in the reaction) with only one resonance peak at 8.6 ppm, is used as an internal standard in these measurements. Each spectrum in Figure 1A is plotted normalized with the internal standard peak keeping at the same magnitude. Two doublets at 7.6 and 6.8 ppm are assigned to meta and ortho protons of the monomer, respectively. With the addition of H₂O₂, the intensities of these two resonance peaks decrease, indicating the monomer is consumed during the polymerization. The residual monomer is calculated by the integration of its ortho proton peak at 6.8 ppm relative to the internal standard peak at 8.6 ppm and plotted as a function of moles of the added H₂O₂ (curve a in Figure 2). The consumption of the monomer increases with the moles of H₂O₂ added in the reaction media. After equal molar H₂O₂ to the monomer is added into the system, close to total conversion is obtained. The data thus appear to validate a stepwise polymerization mechanism as proposed previously,^{2b,5a} where no propagation of radicals exists; each coupling of a growing chain molecule to a monomer molecule requires a molecule of H₂O₂. New peaks from the products of this enzymatic polymerization are also observed in Figure 1A. As expected, the intensities of these peaks are lower compared to that of monomer at the initial stage of the reaction due to their low concentrations. To get a detailed analysis of these weak peaks, the spectra are expanded vertically in Figure 1B. Several interesting features of these NMR spectra are worth noting. First, a strong doublet appears at 6.9 ppm (labeled with asterisks) in the spectrum of the early stage reactions and remains in subsequent spectra. As discussed below, it is believed that this peak is from one of the predominant dimer products formed during the

polymerization. Second, the NMR spectrum becomes complicated with the progress of the reaction. A broad distribution of new resonance peaks is observed in the 6–8 ppm region. This may result from the variation in the structure of the resulted products. Third, the NMR spectrum shows two broad peaks centered at around 6.9 and 7.7 ppm as the reaction proceeds, suggesting the presence of high molecular weight products.

The concentration variation of the predominant dimer product during the reaction is calculated from the integration of the strong doublet at 6.9 ppm relative to the internal standard peak at 8.6 ppm and plotted as a function of the concentration of H₂O₂ (curve b in Figure 2). The process of this peroxidase-catalyzed polymerization reaction may be divided into three different stages based on the variation of the dimer concentration in the system (separated with dotted lines). Stage I is the proliferation of the dimer products. A rapid population growth is observed at early stage of the reaction. The correlation of the conversion of monomers to the growth of dimer population shows that the highest dimer concentration is reached when ca. 33% monomer is converted in the system. The monomers are mainly consumed by the formation of small molecular weight species such as dimers, trimer, etc., at stage I of the reaction. Such a dominance of low molecular weight products at early stage of the reaction is also observed in the experimental and numerical simulation results of peroxidase-catalyzed polymerization of bisphenol A.⁹ Stage II is the dynamic equilibrium of the dimer products. The concentration of dimer products is almost kept at the same concentration level in the system at stage II, though the monomer is continuously being converted. This is an indication that the dimers are also consumed in the reaction to form higher molecular weight products such as trimer and tetramer, etc. It appears that a dynamic equilibrium exists between the formation and consumption of the dimer in the reaction system. The last stage is the reduction of the dimer products (stage III). After the conversion of the monomer is over 70%, the dimer concentration in the system decreases gradually. The dynamic equilibrium of the dimer concentration observed at stage II is altered at this stage. At such a high monomer conversion stage, an enzymatically produced monomer radical has a higher probability to interact with a polymer radical than to interact with another monomer radical to form dimer. Thus, the likelihood for the formation of high molecular weight products increases at this stage. This probably explains a gradual decrease of the dimer concentration during the last stage.

To further confirm our proposed mechanism of this peroxidase-catalyzed polymerization of sulfonated phenols, another reaction was performed where the rates of addition of H₂O₂ and monomer were varied. In this experiment, only the buffer and HRP solution were first transferred to the NMR tube. A stock solution of a mixture of H₂O₂ and monomer (with molar ratio of 1:1) was then added incrementally. NMR spectra were recorded similarly to that described previously. Each of the recorded spectra (data not shown here) shows very similar features to that of the spectra previously recorded at stage III as observed in Figure 1. The peaks at approximately 6.9 ppm, due to the resonance of the formed dimer, were not observed in these spectra. This result is consistent with the proposed reaction mechanism. Because of the presence of equal molar H₂O₂ and

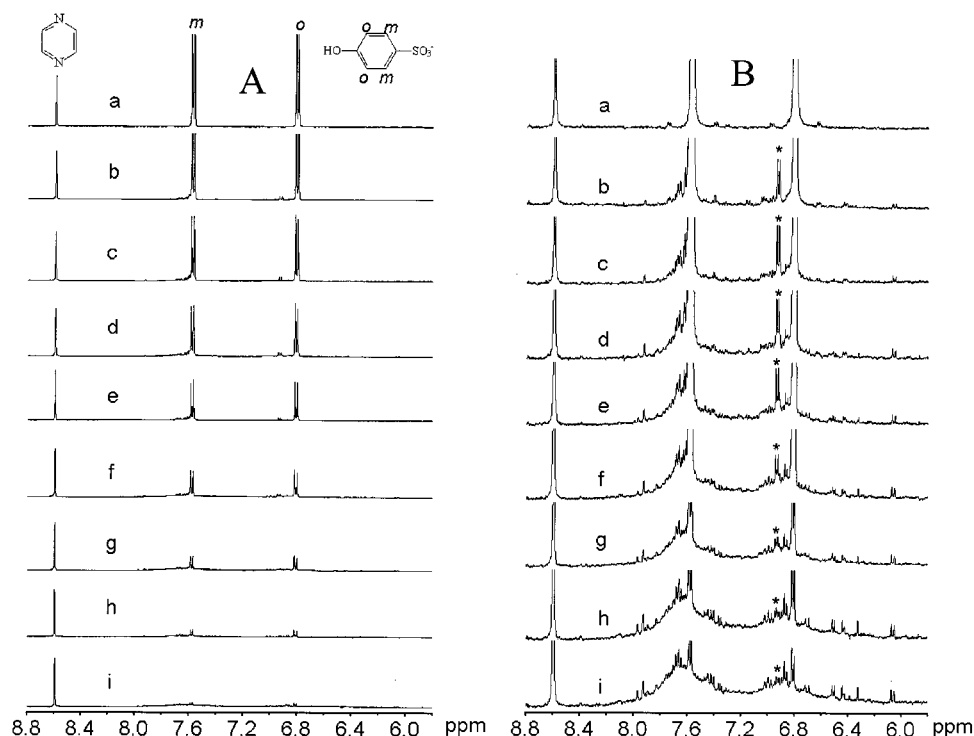


Figure 1. Stack plots of ^1H NMR spectra of the reaction mixture before (a) and after (b–j) incremental addition of H_2O_2 . The molar ratios of the added H_2O_2 to the monomer are (a) 0/8, (b) 1/8, (c) 2/8, (d) 3/8, (e) 4/8, (f) 5/8, (g) 6/8, (h) 7/8, and (i) 8/8. The peak from the internal standard in each spectrum is plotted with the same magnitude in panel A. Panel B is obtained by expanding vertically of the corresponding spectrum in panel A.

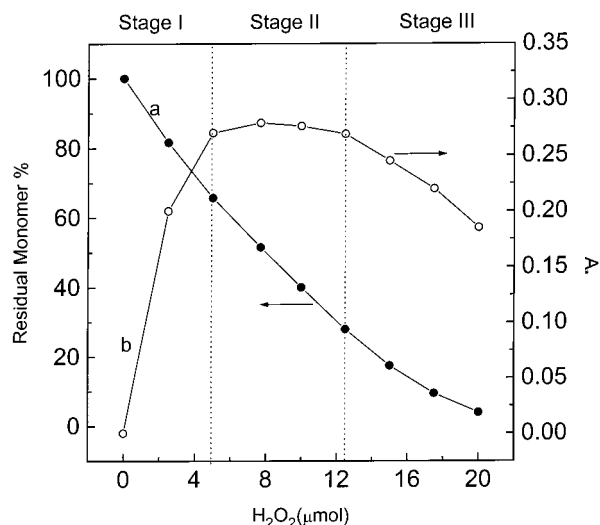


Figure 2. Plots of the residual monomer (%) (a) and the peak integrals (A^*) at 6.9 ppm from the formed dimer product (b) in Figure 1 as a function of the added H_2O_2 . All integrations are performed relative to the internal standard peak which is regarded as 1.

monomer in the solution, the reactions would be expected to progress from stage I to stage III under these conditions. Therefore, each of the NMR spectra should exhibit the features of stage III as observed in Figure 1. Under these conditions, we would expect that the monomers would be totally consumed in the reaction due to the presence of a stoichiometric amount of H_2O_2 . However, the monomer peaks were always observed in the NMR spectra even after long reaction times and with excess H_2O_2 added in the stock solution. The reasons for the presence of this residual monomer are not well understood at this time and are under further investigation.

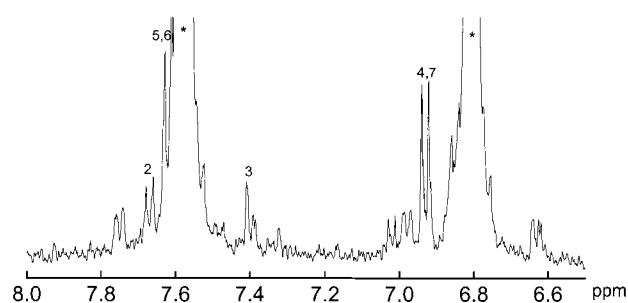


Figure 3. Expanded ^1H NMR spectrum of the reaction mixture at very early stage. The two strong peaks labeled with asterisks are from the monomer.

The peroxidase-catalyzed phenolic polymerization reaction lacks the conventional free radical propagative steps as aforementioned. The major products of the polymerization at an early stage of the peroxidative polymerization are small molecular weight species such as dimer and trimer.⁹ The ^1H NMR spectrum of the reaction mixture at this stage (only $1 \mu\text{mol}$ of H_2O_2 is added, equal to 5% H_2O_2 needed to complete the reaction) is shown in Figure 3. At this very early stage, dimer will be the primary product of the peroxidase-catalyzed polymerization. This is confirmed by determining the relationship between the amount of H_2O_2 and converted monomer in the solution. The calculation, based on the added internal standard (pyrazine), shows that the addition of $1 \mu\text{mol}$ of H_2O_2 resulted in the conversion of approximately $1.9 \mu\text{mol}$ of monomer. This result strongly supports the formation of primarily dimers in the initial stages of the reaction.

Structural characterization of the dimer products formed at the initial stage in the reaction will be helpful to understand the coupling mechanism of the reaction. A set of new resonance peaks is observed clearly in

Scheme 2

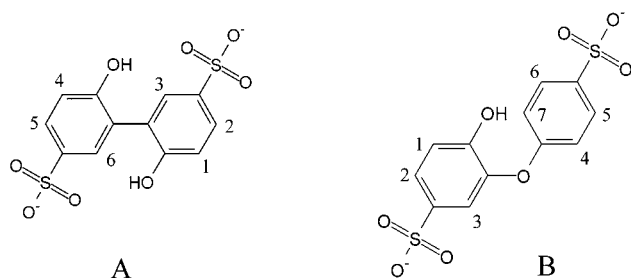


Figure 3. The dominance of the doublet at 6.9 ppm in this early stage spectrum verifies the assignment of this peak from the formed dimer in Figure 1B as we discussed above. Among the four possible monomer coupling reactions for the formation of dimers, two likely occurring dimers are shown in Scheme 2: (1) ortho-ortho carbon coupling to form structure A; (2) C-O-C coupling to form structure B. Since the sulfonated group blocks the para position, the coupling at para position is unlikely. Attempts have been made here to assign some of the resonance peaks for the predominant structures arising from the reaction mixture. The expected ^1H NMR spectrum of structure A will give two doublets at ca. 6.82 (ortho protons; 1,4) and 7.63 ppm (meta protons; 2,5) and one singlet at ca. 7.30 ppm (meta protons; 3, 6) with the same integral according to the spectral calculation. The observed two doublets in Figure 3 at 6.9 and 7.6 ppm with similar intensities could be assigned to the protons 1, 4 and 2, 5, respectively, of structure A. But, the intensity of the observed singlet at 7.4 ppm for the meta proton does not agree with the expected structure A, since it is only half the intensity of the doublet at 6.9 ppm. Therefore, the observed experimental results suggest that the formation of the dimer with structure A is not predominant in the reaction. On the other hand, the pattern of the observed resonance peaks matches with structure B that results from the C-O-C coupling. The possible resonance peak assignment for the different protons from structure B is shown in Figure 3. The ortho protons (4 and 7) of structure B are assigned to the resonance peaks at 6.9 ppm, while the meta protons (5 and 6) to the resonance peaks at 7.6 ppm. The meta protons 3 and 2 of the other phenyl ring are assigned to the singlet resonance peak at 7.4 ppm and to the doublet resonance peak at 7.7 ppm, respectively. The resonance peak of the proton 1 is expected to be slightly upfield compared to the protons 4 and 7 and may be overlapped with the monomer peak at 6.8 ppm. Other minor resonance peaks in Figure 3 arising as a result of enzymatic polymerization are also of interest for a detailed study. Such a detailed study will be reported in future.

The dominance of C-O-C coupling in the reaction suggests that the oxyphenylene rings are the major units in the polymer. This is confirmed by the ^{13}C NMR spectra of this enzymatically synthesized sulfonated polyphenol. The polymers used in these NMR measurements are purified by ultrafiltration as described in Experimental Section. Figure 4 shows the ^{13}C NMR spectra for both the monomer and polymer. Four resonance peaks at 117, 128, 135, and 160 ppm of the monomer are assigned as shown in Figure 4a. The resonance peaks of the polymer (Figure 4b), as expected, are broader. To assist the assignment of the observed ^{13}C NMR resonance peaks of the polymer, ^{13}C NMR DEPT pulse sequence is used for spectral editing. The

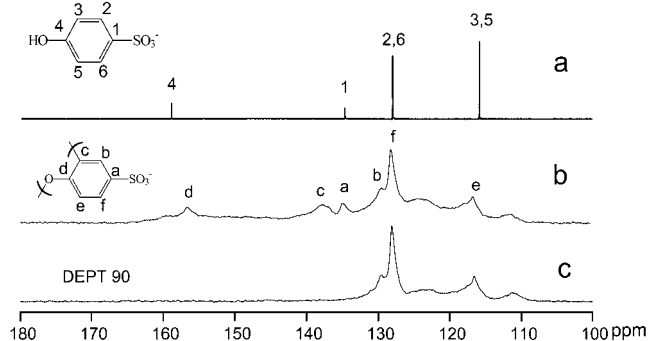


Figure 4. ^{13}C NMR spectra of the monomer (a), polymer (b), and DEPT-90 spectrum of the polymer (c). The structures of the monomer and polymer unit are shown with the possible assignments.

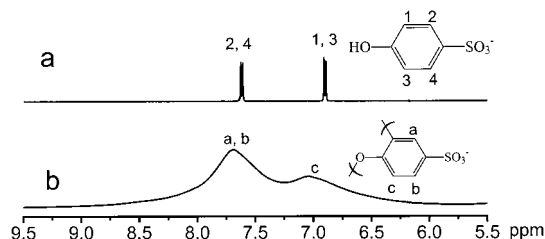


Figure 5. ^1H NMR spectra of the monomer (a) and polymer (b). The structures of the monomer and polymer unit are shown with the possible assignments.

DEPT-90 experiment of the polymer provides a spectrum for ^{13}C resonance of the protonated carbons as shown in Figure 4c. The disappearance of the downfield resonance peaks a, c, and d at 135, 138, and 157 ppm in Figure 4c compared to Figure 4b indicates that these peaks are from nonprotonated aromatic carbons. The assignment of these peaks is shown in Figure 4. The peaks at 138 and 157 ppm are assigned as two different oxy-carbon c and d, and the peak at 135 ppm is from sulfonate group substituted carbon a. The resonance peaks at the upfield region from 110 to 130 ppm are almost identical in Figure 4b,c, suggesting these resonance peaks are from protonated carbons of the polymer. The two peaks at ca. 128 ppm probably are from carbons b and f. The peak at ca. 118 ppm is from carbon e. In contrast to previous observation in peroxidase-catalyzed polymerization of phenol,^{2a} carbon-carbon reaction coupling is not favored in this reaction. Preliminary NMR data analysis suggests the absence of direct carbon-carbon coupling for structure A. (Usually the resonance peaks for C-C coupling carbons appear at 110–130 ppm region^{2f} and should disappear in DEPT-90 spectrum.) It is also possible that the content of the polymer resulted from carbon-carbon coupling reaction may be too low to be detected by ^{13}C NMR techniques. The dominance of C-O-C coupling is also supported by ^1H NMR spectrum of the purified polymer as shown in Figure 5. The spectral features are almost identical with the final stage spectrum (Figure 1B, bottom) that was observed during enzymatic polymerization, except that the sharp peaks arising from the low molecular weight species disappeared in Figure 5. The two broad peaks centered at 6.9 and 7.7 ppm are assigned as shown. This assignment is supported by the integration of these two broad peaks. The integral of the peak at 6.9 ppm is almost half of the peak at 7.7 ppm. Further, the presence of the resonance peak for ortho protons c in ^1H NMR spectrum for the polymer is

consistent with the ^{13}C NMR observation that some of ortho carbons (carbon e in Figure 4) are not participating in the coupling reaction.

Conclusions

In conclusion, the process of HRP-catalyzed polymerization of sulfonated phenol is monitored by ^1H NMR spectroscopy. According to the variation of the dimer concentration during the polymerization, the reaction process may be divided into three different stages: proliferation (I), equilibrium (II), and reduction (III) stages of the dimer. Most conversion of the monomer is devoted to the formation of small molecular weight species such as dimer products at stage I. A dynamic equilibrium exists between the formation and consumption of the dimer in the reaction system at stage II. The likelihood of formation of high molecular weight products increases at high conversion stage of the reaction (stage III). Structural characterization of the predominant dimer products formed at very early stage and the final polymer products suggest that C–O–C coupling is dominant in the polymerization, leading to the synthesis of a polymeric material with sulfonated phenylene oxide as the major unit. Since the peroxidase-catalyzed polymerization of phenol is strongly monomer dependent, detailed investigation on the kinetic process and reaction coupling mechanism of other interesting monomer systems is in progress.

Acknowledgment. The authors gratefully acknowledge the National Science Foundation (NSF) for financial support through research grant DMR-9986644.

References and Notes

- (1) Akkara, J. A.; Kaplan, D. L.; John, V. J.; Tripathy, S. K. In *Polymeric Materials Encyclopedia*; Salamone, J. C., Ed.; CRC Press: Boca Raton, FL, 1996; Vol. 3, D-E, pp 2116–2125.

- (2) (a) Dordick, J. S.; Marletta, M. A.; Klibanov, A. M. *Biotechnol. Bioeng.* **1987**, *30*, 31. (b) Akkara, J. A.; Senecal, K. J.; Kaplan, D. L. *J. Polym. Sci., Part A: Polym. Chem.* **1991**, *29*, 1561. (c) (a) Liu, W.; Bian, S.; Li, L.; Kumar, J.; Samuelson, L. A.; Tripathy, S. K. *Chem. Mater.* **2000**, *12*, 1577. (d) Wang, P.; Dordick, J. S. *Macromolecules* **1998**, *31*, 941. (e) Uyama, H.; Kurioka, H.; Sugihara, J.; Komatsu, I.; Kobayashi, S. *J. Polym. Sci., Part A: Polym. Chem.* **1996**, *35*, 1453. (f) Ayyagar, M. S.; Marx, K. A.; Tripathy, S. K.; Akkara, J. A.; Kaplan, D. L. *Macromolecules* **1995**, *28*, 519.
- (3) (a) Alva, K. S.; Kumar, J.; Marx, K. A.; Tripathy, S. K. *Macromolecules* **1997**, *30*, 4024. (b) Alva, K. S.; Marx, K. A.; Kumar, J.; Tripathy, S. K. *Macromol. Rapid Commun.* **1996**, *17*, 859.
- (4) Liu, W.; Wang, J. D.; Ma, L.; Liu, X. H.; Sun, X. D.; Cheng, Y. H.; Li, T. J. *Ann. N.Y. Acad. Sci.* **1995**, *750*, 138.
- (5) (a) Rao, A. M.; John, V. T.; Gonzalez, R. D.; Akkara, J. A.; Kaplan, D. L. *Biotechnol. Bioeng.* **1993**, *41*, 531. (b) Premachandran, R.; Banerjee, S.; John, V. T.; McPherson, G. L.; Akkara, J. A.; Kaplan, D. L. *Chem. Mater.* **1997**, *9*, 1342. (c) Premachandran, R. S.; Banerjee, S.; Wu, X.-K.; John, V. T.; McPherson, G. L.; Akkara, J. A.; Ayyagari, M.; Kaplan, D. L.; *Macromolecules* **1996**, *29*, 6452.
- (6) Bruno, F.; Akkara, J. A.; Samuelson, L. A.; Kaplan, D. L.; Marx, K. A.; Kumar, J.; Tripathy, S. K. *Langmuir* **1995**, *11*, 889.
- (7) (a) Samuelson, L. A.; Anagnostopoulos, A.; Alva, K. S.; Kumar, J.; Tripathy, S. K. *Macromolecules* **1998**, *31*, 4376. (b) Liu, W.; Kumar, J.; Tripathy, S. K.; Senecal, K. J.; Samuelson, L. A. *J. Am. Chem. Soc.* **1999**, *121*, 71.
- (8) Dunford, H. B. In *Peroxidases in Chemistry and Biology*; Everse, J., Everse, K. E., Grisham, M. B., Eds.; CRC Press: Boca Raton, FL, 1991; Vol. 2, pp 1–24.
- (9) Ryu, K.; McEldoon, J. P.; Pokora, A. R.; Cyrus, W.; Dordick, J. S. *Biotechnol. Bioeng.* **1993**, *42*, 807.
- (10) Alva, K. S.; Samuelson, L.; Kumar, J.; Tripathy, S. K.; Cholli, A. L. *J. Appl. Polym. Sci.* **1998**, *70*, 1257.

MA002006E